fractal and fractional

MDPI

Article

New Bright and Kink Soliton Solutions for Fractional Complex Ginzburg–Landau Equation with Non-Local Nonlinearity Term

Mohammed Alabedalhadi [1], Mohammed Al-Smadi [2,3], Shrideh Al-Omari [4,*], Yeliz Karaca [5] and Shaher Momani [3]

1 Department of Applied Science, Ajloun College, Al-Balqa Applied University, Ajloun 26816, Jordan
2 College of Commerce and Business, Lusail University, Lusail 9717, Qatar
3 Nonlinear Dynamics Research Center (NDRC), Ajman University, Ajman 20550, United Arab Emirates
4 Department of Mathematics, Faculty of Science, Al-Balqa Applied University, Amman 11134, Jordan
5 Umass Chan Medical School, University of Massachusetts (UMASS), 55 Lake Avenue North, Worcester, MA 01655, USA
* Correspondence: shridehalomari@bau.edu.jo; Tel.: +962-772-061-029

Abstract: In this paper, we aim to discuss a fractional complex Ginzburg–Landau equation by using the parabolic law and the law of weak non-local nonlinearity. Then, we derive dynamic behaviors of the given model under certain parameter regions by employing the planar dynamical system theory. Further, we apply the ansatz method to derive soliton, bright and kinked solitons and verify their existence by imposing certain conditions. In addition, we integrate our solutions in appropriate dimensions to explain their behavior at various groups of parameters. Moreover, we compare the graphical representations of the established solutions at different fractional derivatives and illustrate the impact of the fractional derivative on the investigated soliton solutions as well.

Keywords: local fractional derivative; complex Ginzburg–Landau equation; parabolic law; dynamical system; soliton solution

Citation: Alabedalhadi, M.; Al-Smadi, M.; Al-Omari, S.; Karaca, Y.; Momani, S. New Bright and Kink Soliton Solutions for Fractional Complex Ginzburg–Landau Equation with Non-Local Nonlinearity Term. *Fractal Fract.* **2022**, *6*, 724. https://doi.org/10.3390/fractalfract6120724

Academic Editor: Hari Mohan Srivastava

Received: 21 September 2022
Accepted: 5 December 2022
Published: 8 December 2022

1. Introduction

The complex Ginzburg–Landau equation is a type of nonlinear Schrödinger equation, which governs the evolution of certain amplitude of instability pulses in a wide variety of dissipative system. In the literature, many chemical and physical phenomena are described by using the complex Ginzburg–Landau equation, in dynamic phase transitions, surface waves in viscous liquids, processes in optics, laser physics, superconductivity, modeling of Bose–Einstein condensation, spatially extended nonequilibrium systems and other phenomena, to mention but a few (see, e.g., [1–6]). The aforementioned model is also studied by many researchers from several aspects, including phase dynamics and modulation instability. In addition, they extract exact and numerical solutions to this equation (see, e.g., [7–11]). For instance, in [12] the authors obtain soliton solutions to the complex Ginzburg–Landau equation using a modified Jacobi elliptic expansion method. Zayed, E. et al., in [13], investigate optical soliton solutions for the complex Ginzburg–Landau equation (CGLE) with nine different nonlinear forms using two approaches. Moreover, exact solutions for the complex Ginzburg–Landau equation are also constructed with the aid of the planner dynamical system [14]. The authors in [15] present a generalized finite difference method for solving the complex Ginzburg–Landau equation. Díaz, J. et al. in [16], prove the existence and uniqueness of weak solutions for an initial boundary value problem of the complex Ginzburg–Landau equation with some delayed feedback terms. The 2-dimensional stochastic complex Ginzburg–Landau equation and how well-posed the problem is are considered in [17]. Further, the exponential and Kudryashov methods are utilized to obtain 1-soliton solutions for generalization have been considered in [17], as well as proven by the authors of [18].

On the other hand, many studies provide exact and numerical solutions for the fractional complex Ginzburg–Landau equation (FCGLE). In [19], an iterative approach is implemented to find numerical solution for the fractional complex Ginzburg–Landau equation. The authors in [20] introduce a comparative study between three obtained soliton solutions via three fractional derivative definitions. Meanwhile, a study of the dynamics of dissipative solitons for the fractional complex Ginzburg–Landau equation is presented in [21]. An exponential Runge–Kutta technique is adapted to present numerical study for the 2-dimensional nonlinear spatial fractional complex Ginzburg–Landau equation [22]. Lu, P. et al. in [23], obtain exact traveling wave solutions for a (2 + 1)-dimensional fractional complex Ginzburg–Landau equation using the fractional Riccati and bifunction method. The authors in [24] introduce a 3-level linearized implicit difference scheme for the 2-dimensional spatial fractional complex Ginzburg–Landau equation. They also show under mild conditions that the proposed approach is uniquely solvable, convergent and stable as well. The fractional complex Ginzburg–Landau equation in three spatial dimensions with the dissipative effect are studied in [25]. In this citation, authors construct a prior estimate under certain growth conditions. Moreover, they also present the existence and uniqueness of a global smooth solution. Huang and Li in [26] utilize the complete discrimination system technique to development exact solutions of the fractional complex Ginzburg–Landau equation in the sense of the conformable fractional derivative.

Hereafter, we consider the following model:

$$\begin{aligned} i\frac{\partial^{\eta}\psi}{\partial t^{\eta}} + a_1\frac{\partial^{2\eta}\psi}{\partial x^{2\eta}} + \left(q_1|\psi|^2 + q_2|\psi|^4 + q_3\frac{\partial^{2\eta}|\psi|^2}{\partial x^{2\eta}}\right)\psi \\ = a_2\frac{\left|\frac{\partial^{\eta}\psi}{\partial x^{\eta}}\right|^2}{\psi^*} + \frac{a_3}{4|\psi|^2\psi^*}\left(2|\psi|^2\frac{\partial^{2\eta}|\psi|^2}{\partial x^{2\eta}} - \left(\frac{\partial^{2\eta}|\psi|^2}{\partial x^{2\eta}}\right)^2\right) + a_4\psi, \end{aligned} \tag{1}$$

where the parameter a_1 represents the group velocity dispersion, a_2 and a_3 represent perturbation effects, a_4 symbolizes the detuning effect, q_1 and q_2 are assigned to the parabolic law, while q_3 represents the nonlocal nonlinearity term. The independent variables x and t symbolize the nondimensional distance along the fiber and time in dimensionless form, respectively. The complex-valued function $\psi = \psi(t, x)$ constitutes the wave profile, while $\psi^*(t, x)$ is assigned to its conjugate. However, the novelty of this paper is to investigate bright and kink soliton solutions using the ansatz method for the governing model (1) and study its dynamic behavior using the theory of the dynamic planner system [27–34]. In this paper, the ansatz method is utilized for the first time to establish wave solutions for the fractional complex Ginzburg–Landau equation with non-local nonlinearity term. There exists no work in the literature, as far as we know, that considers the fractional complex Ginzburg–Landau equation in local fractional derivative sense. Therefore, all constructed solutions in this paper are new and are displayed in graphical representations to illustrate their physical properties.

This paper is arranged as follows: an overview of needful concepts is given in Section 2. Section 3 is dedicated to utilizing a suitable traveling wave transformation on (1) to reduce it into an integer-order ordinary differential equation. In Section 4, we introduce the equilibria classification for the obtained dynamic system. The bright solitons and kink solitons solutions for (1) have been established in Section 5. Several concluding remarks are listed in Section 6.

2. Preliminaries

We dedicate this section to present an overview of needful concepts in our work. The definition of the local fractional derivatives (LFD) and their properties have been listed in the paper. For function $\psi(\zeta) \in \mathcal{C}_{\eta}(a, b)$ and $\varepsilon > 0$, there is $\delta > 0$ such that $|\psi(\zeta) - \psi(\zeta_0)| < \varepsilon^{\eta}$ holds for $|\zeta - \zeta_0| < \delta$, where $\varepsilon, \delta \in \mathbb{R}$.

Definition 1 ([35]). *Let $\eta \in (0,1)$ and $\psi(\zeta) \in \mathcal{C}_\eta(a,b)$. Then, the local fractional derivative of order of the function $\psi(\zeta)$ at the point $\zeta = \zeta_0$ is defined as*

$$\mathcal{D}_\zeta^\eta \psi(\zeta_0) = \frac{d^\eta \psi(\zeta_0)}{d\zeta^\eta} = \lim_{\zeta \to \zeta_0} \frac{\Delta^\eta(\psi(\zeta) - \psi(\zeta_0))}{(\zeta - \zeta_0)^\eta}, \tag{2}$$

where Δ^η is an operator defined as:

$$\Delta^\eta(\psi(\zeta) - \psi(\zeta_0)) \cong \Gamma(1+\eta)\Delta(\psi(\zeta) - \psi(\zeta_0)). \tag{3}$$

The following theorem presents the substantial properties of the local fractional derivatives.

Theorem 1 ([35]). *Let $\eta \in (0,1)$ and $\psi_1(\zeta),\ \psi_2(\zeta) \in \mathcal{C}_\eta(a,b)$. Then, the attached properties are attained:*

$$(p1)\ \mathcal{D}_\zeta^\eta[\psi_1(\zeta) \pm \psi_2(\zeta)] = \mathcal{D}_\zeta^\eta \psi_1(\zeta) \pm \mathcal{D}_\zeta^\eta \psi_2(\zeta),$$

$$(p2)\ \mathcal{D}_\zeta^\eta[\psi_1(\zeta)\psi_2(\zeta)] = \mathcal{D}_\zeta^\eta(\psi_1(\zeta))\psi_2(\zeta) + \psi_1(\zeta)\mathcal{D}_\zeta^\eta \psi_2(\zeta),$$

$$(p3)\ \mathcal{D}_\zeta^\eta\left[\frac{\psi_1(\zeta)}{\psi_2(\zeta)}\right] = \frac{\mathcal{D}_\zeta^\eta(\psi_1(\zeta))\psi_2(\zeta) - \psi_1(\zeta)\mathcal{D}_\zeta^\eta \psi_2(\zeta)}{(\psi_2(\zeta))^2},\ \psi_2(\zeta) \neq 0.$$

$$(p4)\ \mathcal{D}_\zeta^\eta[\psi_1(\zeta) \circ \psi_2(\zeta)] = \mathcal{D}_\zeta^\eta \psi_1(\psi_2(\zeta))\left(\psi_2^{(1)}(\zeta)\right)^\eta = \psi_1^{(1)}(\psi_2(\zeta))\mathcal{D}_\zeta^\eta \psi_2(\zeta).$$

$$(p5)\ \mathcal{D}_\zeta^\eta \zeta^{n\eta} = \frac{\Gamma(1+n\eta)}{\Gamma(1+(n-1)\eta)}\zeta^{(n-1)\eta}.$$

Definition 2 ([35]). *Let $\eta \in (0,1)$. Then, the local fractional partial derivative (LFPD) of the fractal function $\psi(\zeta,\theta)$ of the fractional order η, at the point $\zeta = \zeta_0$ is defined as*

$$\mathcal{D}_\zeta^\eta \psi(\zeta_0,\theta) = \frac{\partial^\eta \psi(\zeta_0,\theta)}{\partial\zeta^\eta} = \lim_{\zeta \to \zeta_0} \frac{\Delta^\eta(\psi(\zeta,\theta) - \psi(\zeta_0,\theta))}{(\zeta - \zeta_0)^\eta}, \tag{4}$$

where Δ^η is an operator defined as:

$$\Delta^\eta(\psi(\zeta,\theta) - \psi(\zeta_0,\theta)) \cong \Gamma(1+\eta)\Delta(\psi(\zeta,\theta) - \psi(\zeta_0,\theta)). \tag{5}$$

The local fractional partial derivative of $\psi(\zeta,\theta)$ at $\theta = \theta_0$ can be defined in a similar way. The reader can be referred to [35–39] for more details about the local fractional calculus.

3. Transformation and Hamiltonian

In this section, we utilize a suitable traveling wave transformation to reduce (1) into an integer-order ordinary differential equation (ODE). Then, we introduce the corresponding dynamic system and its Hamiltonian. For this purpose, the same technique used in [40–42] is applied, in which the following complex fractional traveling wave transformation [43] is considered:

$$\psi(t,x) = \Psi(\chi)e^{(i(\frac{\gamma(t-t_0)^\eta}{\Gamma(1+\eta)} + \frac{\delta(x-x_0)^\eta}{\Gamma(1+\eta)}))},\ \chi = \frac{\alpha}{\Gamma(1+\eta)}(t-t_0)^\eta + \frac{\beta}{\Gamma(1+\eta)}(x-x_0)^\eta, \tag{6}$$

where Ψ is the amplitude of the wave profile, α represents the soliton speed, δ is the frequency of the soliton and γ is assigned to be the soliton wave number. Employing the

transformation given in (6) and using the chain rule of the LFD, we achieve the following relations:

$$\frac{\partial^{\eta}\psi}{\partial t^{\eta}} = \left(\alpha\frac{d\Psi}{d\chi} + i\gamma\Psi\right)e^{\left(i\left(\frac{\gamma}{\Gamma(1+\eta)}t^{\eta}+\frac{\delta}{\Gamma(1+\eta)}x^{\eta}\right)\right)}, \tag{7}$$

$$\frac{\partial^{2\eta}\psi}{\partial x^{2\eta}} = \left(\beta^2\frac{d^2\Psi}{d\chi^2} + 2i\beta\delta\frac{d\Psi}{d\chi} - \delta^2\Psi\right)e^{\left(i\left(\frac{\gamma}{\Gamma(1+\eta)}t^{\eta}+\frac{\delta}{\Gamma(1+\eta)}x^{\eta}\right)\right)}, \tag{8}$$

$$\frac{\partial^{\eta}|\psi|^2}{\partial x^{\eta}} = 2\beta\Psi\frac{d\Psi}{d\chi}, \tag{9}$$

$$\frac{\partial^{2\eta}|\psi|^2}{\partial x^{2\eta}} = 2\beta^2\left(\left(\frac{d\Psi}{d\chi}\right)^2 + \Psi\frac{d^2\Psi}{d\chi^2}\right), \tag{10}$$

$$\left|\frac{\partial^{\eta}\psi}{\partial x^{\eta}}\right|^2 = \left(\beta\frac{d\Psi}{d\chi} + i\delta\Psi\right)^2. \tag{11}$$

Substitute the relations in (7)–(11) into the commanding model (1) to acquire the following complex ODE:

$$\begin{aligned} &i\left(\alpha\tfrac{d\Psi}{d\chi} + i\gamma\Psi\right) + a_1\left(\beta^2\tfrac{d^2\Psi}{d\chi^2} + 2i\beta\delta\tfrac{d\Psi}{d\chi} - \delta^2\Psi\right)\\ &\quad+\Psi\left(q_1\Psi^2 + q_2\Psi^4 + q_3\left(2\beta^2\left(\left(\tfrac{d\Psi}{d\chi}\right)^2 + \Psi\tfrac{d^2\Psi}{d\chi^2}\right)\right)\right)\\ &\quad= a_2\tfrac{1}{\Psi}\left(\beta\tfrac{d\Psi}{d\chi} + i\delta\Psi\right)^2\\ &\quad+\tfrac{a_3}{4\Psi^3}\left(2\Psi^2\left(2\beta^2\left(\left(\tfrac{d\Psi}{d\chi}\right)^2 + \Psi\tfrac{d^2\Psi}{d\chi^2}\right)\right) - \left(2\beta\Psi\tfrac{d\Psi}{d\chi}\right)^2\right) + a_4\Psi. \end{aligned} \tag{12}$$

The velocity of the soliton can be obtained from the imaginary part of the complex Equation (12). It reads as:

$$\alpha = -2a_1\beta\gamma. \tag{13}$$

The real part of the complex Equation (12) is written as:

$$\begin{aligned} &\left(a_2\delta^2 - a_1\delta^2 - a_4 - \gamma\right)\Psi^2 + q_1\Psi^4 + q_2\Psi^6 - a_2\beta^2\left(\tfrac{d\Psi}{d\chi}\right)^2 + 2q_3\beta^2\Psi^2\left(\tfrac{d\Psi}{d\chi}\right)^2\\ &\quad+\beta^2(a_1 - a_3)\Psi\tfrac{d^2\Psi}{d\chi^2} + 2q_3\beta^2\Psi^3\tfrac{d^2\Psi}{d\chi^2} = 0. \end{aligned} \tag{14}$$

Let $\frac{d\Psi}{d\chi} = \Phi$. Then, Equation (14) is equivalent to the following dynamic system:

$$\begin{aligned} \tfrac{d\Psi}{d\chi} &= \Phi,\\ \tfrac{d\Phi}{d\chi} &= -\tfrac{\left(a_2\delta^2 - a_1\delta^2 - a_4 - \gamma\right)\Psi^2 + q_1\Psi^4 + q_2\Psi^6 - a_2\beta^2\Phi^2 + 2q_3\beta^2\Psi^2\Phi^2}{\beta^2(a_1 - a_3)\Psi + 2q_3\beta^2\Psi^3}. \end{aligned} \tag{15}$$

The Hamiltonian function [44,45] is given for the dynamic system (15) as:

$$\begin{aligned} \mathcal{H}(\Psi,\Phi) &= \tfrac{1}{3}\left(a_2\delta^2 - a_1\delta^2 - a_4 - \gamma\right)\Psi^3 + \tfrac{1}{5}q_1\Psi^5 + \tfrac{1}{7}q_2\Psi^7 + \tfrac{\beta^2}{2}(a_1 - 2a_2 - a_3)\Psi\Phi^2\\ &\quad+\tfrac{5q_3\beta^2}{3}\Psi^3\Phi^2 = \Delta. \end{aligned} \tag{16}$$

As the phase orbits (15) decides the traveling wave solutions of equation (1), one can examine bifurcations of the phase profiles of Equation (15) in the (Ψ,Φ) phase plane. A solitary wave solution of Equation (1) is analogous to a homoclinic orbit of Equation (15). A periodic orbit of Equation (15) corresponds to a periodic traveling wave solution of Equation (1).

4. Equilibria Classification

The regular system associated with the dynamic system (15) is given as

$$\begin{aligned} \frac{d\Psi}{d\xi} &= \left(\beta^2(a_1-a_3)\Psi + 2q_3\beta^2\Psi^3\right)\Phi, \\ \frac{d\Phi}{d\xi} &= -\left(a_2\delta^2 - a_1\delta^2 - a_4 - \gamma\right)\Psi^2 - q_1\Psi^4 - q_2\Psi^6 + a_2\beta^2\Phi^2 - 2q_3\beta^2\Psi^2\Phi^2, \end{aligned} \tag{17}$$

which has the same Hamiltonian function as (15), where $d\chi = \left(\beta^2(a_1-a_3)\Psi + 2q_3\beta^2\Psi^3\right)d\xi$.

Obviously, all equilibrium points for (17) lie on the Ψ-axes on the (Ψ, Φ)-plane.

Let $\Delta = q_1^2 - 4q_2\left(a_2\delta^2 - a_1\delta^2 - a_4 - \gamma\right)$. Then, the equilibrium points for the dynamic system (17) can be obtained under the following assumptions:

Case 1. If $q_1 < 0$, $a_2\delta^2 - a_1\delta^2 - a_4 - \gamma > 0$, and $\Delta = 0$, then there are three equilibrium points:

$$\mathcal{E}_1(0,0) \text{ and } \mathcal{E}_{2,3}\left(\pm\sqrt{-\frac{2(a_2\delta^2 - a_1\delta^2 - a_4 - \gamma)}{q_1}}, 0\right).$$

Case 2. If $q_1 > 0$, $a_2\delta^2 - a_1\delta^2 - a_4 - \gamma < 0$, and $\Delta = 0$, then there are three equilibrium points:

$$\mathcal{E}_1(0,0) \text{ and } \mathcal{E}_{2,3}\left(\pm\sqrt{-\frac{2(a_2\delta^2 - a_1\delta^2 - a_4 - \gamma)}{q_1}}, 0\right).$$

Case 3. If $q_2 > 0$, $\left(a_2\delta^2 - a_1\delta^2 - a_4 - \gamma\right) < 0$, and $\Delta > 0$, then there are three equilibrium points:

$$\mathcal{E}_1(0,0) \text{ and } \mathcal{E}_{2,3}\left(\pm\sqrt{\frac{-q_1 + \sqrt{\Delta}}{2q_2}}, 0\right).$$

Case 4. If $q_2 < 0$, $\left(a_2\delta^2 - a_1\delta^2 - a_4 - \gamma\right) > 0$, and $\Delta > 0$, then there are three equilibrium points:

$$\mathcal{E}_1(0,0) \text{ and } \mathcal{E}_{2,3}\left(\pm\sqrt{\frac{-q_1 + \sqrt{\Delta}}{2q_2}}, 0\right).$$

Case 5. If $q_2 < 0$, $\Delta > 0$, and $q_1 > 0$, then there are three equilibrium points:

$$\mathcal{E}_1(0,0) \text{ and } \mathcal{E}_{2,3}\left(\pm\sqrt{\frac{-q_1 - \sqrt{\Delta}}{2q_2}}, 0\right).$$

Case 6. If $q_2 < 0$, $\left(a_2\delta^2 - a_1\delta^2 - a_4 - \gamma\right) < 0$, and $\Delta > 0$, then there are five equilibrium points:

$$\mathcal{E}_1(0,0) \text{ and } \mathcal{E}_{2,3,4,5}\left(\pm\sqrt{\frac{-q_1 \pm \sqrt{\Delta}}{2q_2}}, 0\right).$$

Case 7. If $q_2 > 0$, $\left(a_2\delta^2 - a_1\delta^2 - a_4 - \gamma\right) > 0$, and $\Delta > 0$, then there are five equilibrium points:

$$\mathcal{E}_1(0,0) \text{ and } \mathcal{E}_{2,3,4,5}\left(\pm\sqrt{\frac{-q_1 \pm \sqrt{\Delta}}{2q_2}}, 0\right).$$

Let $M(\mathcal{E}^*)$ be the coefficient matrix of the linearized system (17) at equilibrium point $\mathcal{E}^*$. Define:

$$\mathcal{J}(\mathcal{E}^*) = \det(\mathcal{M}(\mathcal{E}^*)). \tag{18}$$

Let $\sigma = a_4 + \gamma + (a_1 - a_2)\delta$ and $\Psi_0 = 0$, $\Psi_1^{\pm} = \pm\sqrt{-\frac{\sqrt{-4q_2\sigma}}{2q_2}}$, $\Psi_2^{\pm} = \pm\sqrt{\frac{\sqrt{-4q_2\sigma}}{2q_2}}$, $\Psi_3^{\pm} = \pm\sqrt{\frac{-q_1+\sqrt{\Delta}}{2q_2}}$, and $\Psi_4^{\pm} = \pm\sqrt{\frac{-q_1-\sqrt{\Delta}}{2q_2}}$.

Then, we get:

$$\mathcal{J}(\Psi_0, 0) = 0, \tag{19}$$

$$\mathcal{J}(\Psi_1^{\pm},0) = \frac{1}{q_2^2\sqrt{\frac{\sigma}{\sqrt{-q_2\sigma}}}}(-2\beta^2\sigma(q_2(a_2-a_1)+2q_3\sqrt{-q_2\sigma}) \times(\pm\sigma+(-2q_1+3\sqrt{-q_2\sigma})\sqrt{\frac{\sigma}{\sqrt{-q_2\sigma}}})), \tag{20}$$

$$\mathcal{J}(\Psi_2^{\pm},0) = \frac{1}{q_2^2\sqrt{\frac{\sqrt{-q_2\sigma}}{q_2}}}(2\beta^2\sigma(q_2(a_1-a_2)+2q_3\sqrt{-q_2\sigma}) \times(\pm\sigma-(2q_1+3\sqrt{-q_2\sigma})\sqrt{\frac{\sqrt{-q_2\sigma}}{q_2}})), \tag{21}$$

$$\mathcal{J}(\Psi_3^{\pm},0) = \frac{1}{4q_2^3}(\beta^2(\sqrt{\Delta}-q_1)(q_2(a_1-a_2)+(\sqrt{\Delta}-q_1)q_3) \times(3\Delta-2\sqrt{\Delta}q_1-q_1^2\mp 2\sqrt{2}q_2\sigma\sqrt{\frac{\sqrt{\Delta}-q_1}{q_2}})), \tag{22}$$

$$\mathcal{J}(\Psi_4^{\pm},0) = \frac{1}{4q_2^3}(\beta^2(\sqrt{\Delta}+q_1)(q_2(a_2-a_1)+(\sqrt{\Delta}+q_1)q_3) \times(3\Delta+2\sqrt{\Delta}q_1-q_1^2\mp 2\sqrt{2}q_2\sigma\sqrt{\frac{-\sqrt{\Delta}-q_1}{q_2}})). \tag{23}$$

We have classified the gained equilibrium point $\mathcal{E}^*$ of the system (17) using the planar dynamic system theory as follows: if $\mathcal{J} > 0$, then the point is center. The point is said to be saddle if $\mathcal{J} < 0$ and the point is cusp if $\mathcal{J} = 0$, provided the poincare index of the equilibrium point is zero [44,45], see also [29–34,46–48] for further details. The phase portrait for the system (17) is shown in Figures 1–4. Figure 1 presents the phase portrait when the system has three equilibrium points according to cases 1 and 2, provided the equilibria $\mathcal{E}_1(0,0)$ is cuspidal point. Figure 1b presents two family of open curves that tend to the singular line $\Psi = 0$ when $|\Phi| \to \infty$. In Figure 2a, the phase portrait shows a nonlinear periodic trajectory located at centers $\mathcal{E}_{2,3}(\Psi_3^{\pm},0)$, while it shows a set of families of open curves around the saddle points $\mathcal{E}_{2,3}(\Psi_3^{\pm},0)$ in Figure 2b. In Figure 3a, the level curves surrounding the point $\mathcal{E}_1(0,0)$ correspond to a family of periodic orbits of the system (17), while there are two heteroclinic orbits surrounding $\mathcal{E}_1(0,0)$ and connect the saddle equilibria points $\mathcal{E}_{2,3}(\Psi_4^{\pm},0)$. The curves presented in Figure 3b show a nonlinear periodic trajectory located at centers $\mathcal{E}_{2,3}(\Psi_4^{\pm},0)$. Figure 4a,b shows five equilibria points for the system (17) that correspond to Case 6 and 7. In Figure 4a, there is a homoclinic trajectory at the saddle points $\mathcal{E}_{2,3}(\Psi_3^{\pm},0)$ enclosing the centers $\mathcal{E}_{4,5}(\Psi_4^{\pm},0)$. Figure 4b shows a homoclinic trajectory at the saddle points $\mathcal{E}_{4,5}(\Psi_4^{\pm},0)$ enclosing the centers $\mathcal{E}_{2,3}(\Psi_3^{\pm},0)$.

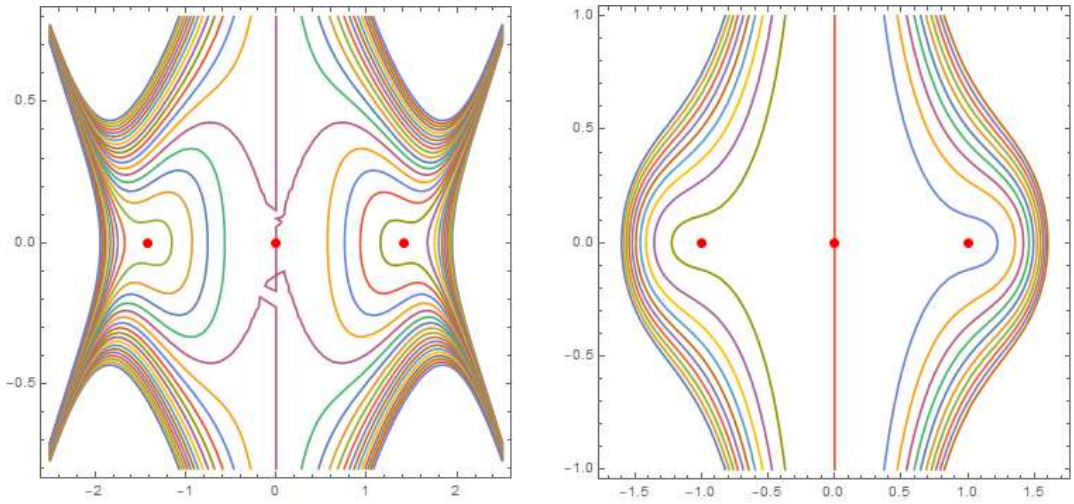

(**a**) (**b**)

Figure 1. Trajectories of the dynamical system (17), where (**a**) $a_1 = 1, a_2 = 0, a_4 = 0, q_1 = 2, q_3 = 1, \gamma = 1, \delta = 1, \beta = 1, q_2 = -\frac{(q_1)^2}{4\sigma}$; (**b**) $a_1 = 0, a_2 = 0, a_4 = 0, q_1 = -2, q_3 = 1, \gamma = -1, \delta = 1, \beta = 1, q_2 = -\frac{(q_1)^2}{4\sigma}$.

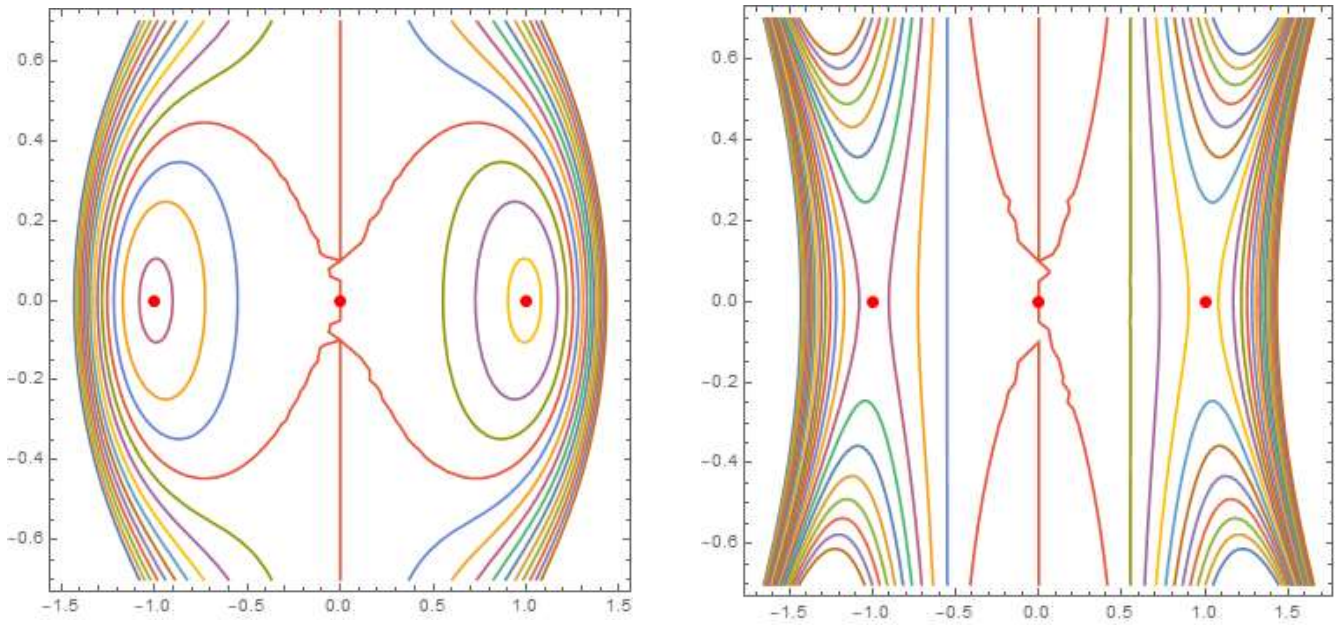

(**a**) (**b**)

Figure 2. Trajectories of the dynamical system (17), where (**a**) $a_1 = 1, a_2 = 0, a_4 = 0, q_1 = 1, q_2 = 1, q_3 = 1, \gamma = 1, \delta = 1, \beta = 1$; (**b**) $a_1 = 1, a_2 = 0, a_4 = 0, q_1 = 1, q_2 = 1, q_3 = -1, \gamma = 1, \delta = 1, \beta = 1$.

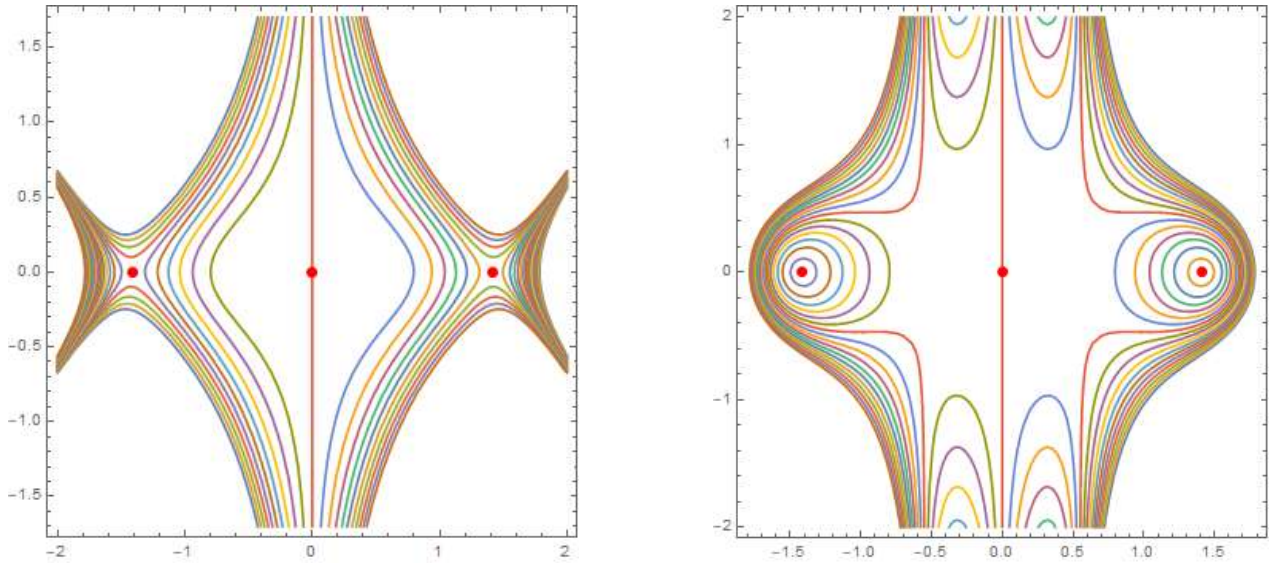

(**a**) (**b**)

Figure 3. Trajectories of the dynamical system (17), where (**a**) $a_1 = 1, a_2 = 0, a_4 = 0, q_1 = 2, q_2 = -1, q_3 = 1; \gamma = -1, \delta = 1, \beta = 1$; (**b**) $a_1 = 1, a_2 = 0, a_4 = 0, q_1 = 2, q_2 = -1, q_3 = -1, \gamma = -1, \delta = 1, \beta = 1$.

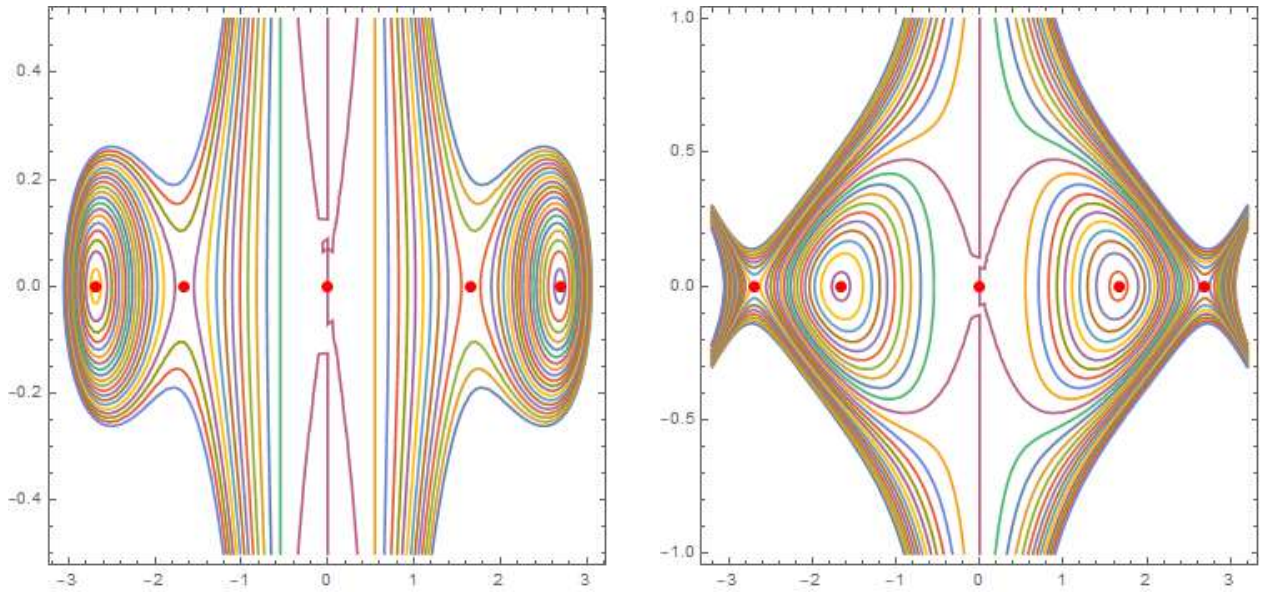

(**a**) (**b**)

Figure 4. Trajectories of the dynamical system (17), where (**a**) $a_1 = 1, a_2 = 0, a_4 = 0, q_1 = 1, q2 = -0.1, q3 = -1, \gamma = 1, \delta = 1, \beta = 1$; (**b**) $a_1 = 1, a_2 = 0, a_4 = 0, q_1 = 1, q_2 = -0.1, q_3 = 1, \gamma = 1, \delta = 1, \beta = 1$.

5. Bright and Kink Wave Solutions

Usually, the existence of heteroclinic, homoclinic and periodic orbits for the system (17) correspond to the existence of kink, solitary (bright or dark) and periodic wave solutions for the governing model (1). Therefore, using the ansatz method, we will construct bright and kink wave solutions for the governing model (1).

5.1. Bright Soliton

To demonstrate a bright soliton solution for Equation (1), we assume the solution for the obtained ordinary differential Equation (14) has the form:

$$\Psi(\chi) = \frac{\mathcal{A}\operatorname{sech}(m\chi)}{\sqrt{1 + \mathcal{B}\operatorname{sech}^2(m\chi)}}, \tag{24}$$

where A, $\mathcal{B}$ and m are constants to be determined. Substituting (24) into (14), simplifying the result and grouping the coefficients of the linearly independent terms, then setting it to be zero, yields a nonlinear algebraic system that has the following solution:

$$\mathcal{A} \text{ and } \mathcal{B} \text{ are arbitrary, } \gamma = a_4 + a_1\delta^2, a_3 = a_1, a_2 = 0, q_1 = 0, q_3\beta \neq 0, m = \pm\frac{A}{\beta}\sqrt{\frac{q_2}{2q_3}},\ q_2q_3 > 0. \tag{25}$$

Inserting the result of (25) into (24), then using it with (6), the bright soliton solutions for the commanding model (1) can be introduced as follows:

$$\begin{aligned}\psi_{1,2}(t,x) = {} & \frac{\mathcal{A}\operatorname{sech}(\pm\frac{\mathcal{A}}{\Gamma(1+\eta)}\sqrt{\frac{q_2}{2q_3}}(x^\eta - 2a_1(a_4+a_1\delta^2)t^\eta))}{\sqrt{1+\mathcal{B}\operatorname{sech}^2(\pm\frac{\mathcal{A}}{\Gamma(1+\eta)}\sqrt{\frac{q_2}{2q_3}}(x^\eta - 2a_1(a_4+a_1\delta^2)t^\eta))}} \\ & \times e^{(i(\frac{(a_4+a_1\delta^2)}{\Gamma(1+\eta)}t^\eta + \frac{\delta}{\Gamma(1+\eta)}x^\eta))}.\end{aligned} \tag{26}$$

Figure 5 shows the 3D plot of the obtained solution of (26), $|\psi_1(x,t)|$, where we consider the case when $m = \frac{A}{\beta}\sqrt{\frac{q_2}{2q_3}}$, at selected parameters, with the spatial variable $x \in [-25, 25]$ and the temporal variable $t \in [0, 3]$. To show the effect of the fractional

derivative on the behavior of the soliton solution, a comparison between the soliton solution at integer-order and fractional-order has been considered in Figure 5a,b.

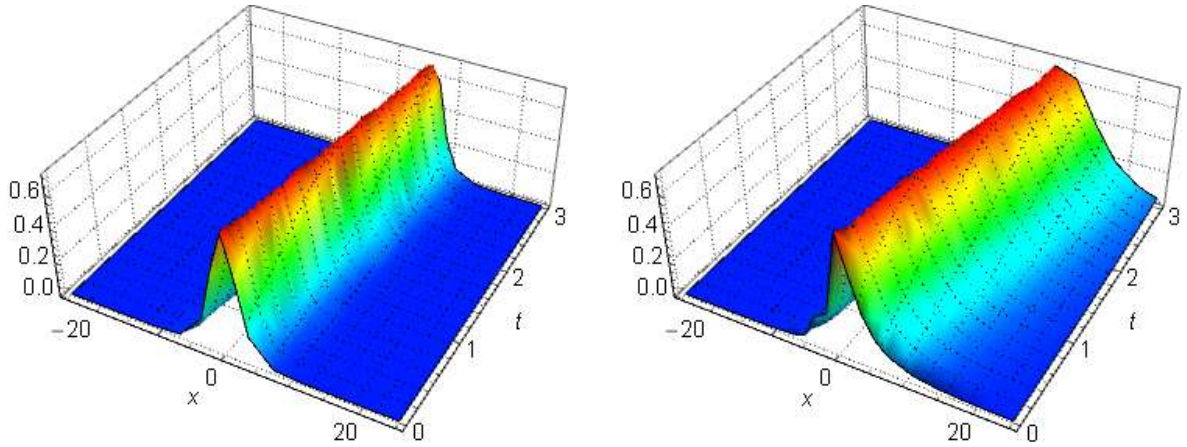

(**a**) (**b**)

Figure 5. Bright soliton solution (26), $|\psi_1(x,t)|$, where $m = \frac{A}{\beta}\sqrt{\frac{q_2}{2q_3}}$, for (1) at $A = \mathcal{B} = a_1 = q_2 = q_3 = \gamma = 1$, $a_4 = 0$: (**a**) integer derivative order $\eta = 1$; (**b**) fractional derivative order $\eta = 0.68$.

For more details about the effectiveness of the fractional order on the solution, we present a comparison between the obtained solution $\psi_1(x,t)$ in (26) at various fractional derivative orders, see Figure 6. The change in the order of the fractional derivative is accompanied by a change in the width of the inferred wave, and sometimes the wave shape changes completely. For example, when the derivative is $\eta = 0.4$, the soliton solution is not entirely bright.

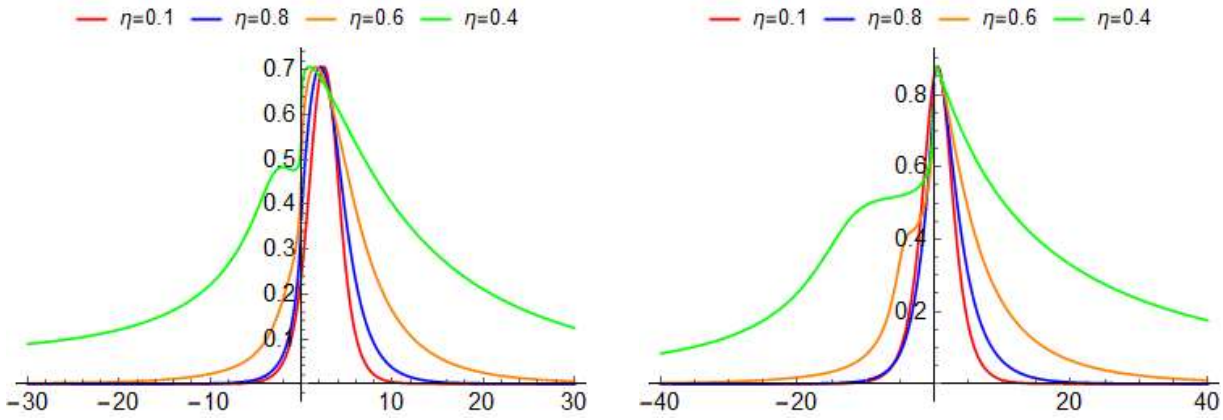

(**a**) (**b**)

Figure 6. Bright soliton solution (26), $|\psi_1(x,t)|$, where $m = \frac{A}{\beta}\sqrt{\frac{q_2}{2q_3}}$, for (1) at: (**a**) 2D plot where $t = 5$, $\mathcal{A} = \mathcal{B} = a_1 = 1, q_2 = 1.8$, $q_3 = 1.3, \gamma = 0.5$, $a_4 = 0$; (**b**) 2D plot where $t = 1$, $\mathcal{A} = 1$, $\mathcal{B} = 0.3$, $a_1 = 1, q_2 = 0.8$, $q_3 = 1.3, \gamma = 0.5$, $a_4 = 0$.

Moreover, we have studied the variation of the inferred solution (26) with the group velocity dispersion parameter a_1 and detuning effect parameter a_4 in Figure 7a,b, respectively.

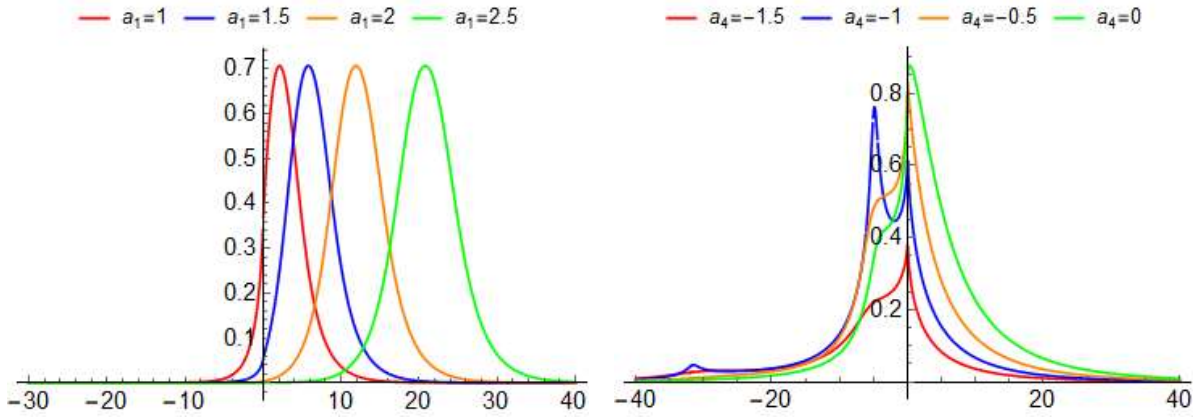

(**a**) (**b**)

Figure 7. Variation of the inferred bright soliton solution (26), $|\psi_2(x,t)|$, where $m = -\frac{A}{\beta}\sqrt{\frac{q_2}{2q_3}}$ for (1): (**a**) with the group velocity dispersion parameter a_1 where: $A = \mathcal{B} = a_1 = 1, q_2 = 1.8,\ q_3 = 1.3,$ $\gamma = 0.5,\ a_4 = 0$ and $t = 5$; (**b**) detuning effect parameter a_4 where: $A = 1,\ \mathcal{B} = 0.3,\ a_1 = 1,$ $q_2 = 0.8,\ q_3 = 1.3, \gamma = 0.5,\ a_4 = 0$ and $t = 1$.

5.2. Kink Soliton

To construct a kink soliton solution for the governing model (1), the solution for the integer-order ordinary differential Equation (14) assumes the form:

$$\Psi(\chi) = \mathcal{A}\sqrt{1 + \tanh(m\chi)}. \tag{27}$$

Substituting the formal solution of (27) into the integer-order ODE (14), we, after simplification, get an expression with linearly independent terms, namely, $\tanh^i(m\chi), \operatorname{sech}^j(m\chi)$ and $\tanh^k(m\chi)\operatorname{sech}^2(m\chi)$, where $i = 1,2,3,4,\ j = 2,4$ and $k = 1,2$, in addition to the fixed term. If the coefficients of these linearly independent terms vanish, we get an overdetermined nonlinear algebraic system, and its solution sets are listed in the following cases:

Case 1. If $q_1 \neq 0,\ a_2\beta \neq 0,\ a_1 = a_3,\ q_3 = 0,\ q_2 = \frac{-q_1^2}{4(a_4+\gamma+(a_1-a_2)\delta)}$, $q_1(a_4 + \gamma + (a_1 - a_2)\delta) > 0$ and $a_2(a_4 + \gamma + (a_1 - a_2)\delta) < 0$, then:

$$\mathcal{A}_{1,2} = \pm\sqrt{\frac{a_4 + \gamma + (a_1 - a_2)\delta}{q_1}},\ m_{1,2} = \pm\sqrt{\frac{-(a_4 + \gamma + (a_1 - a_2)\delta)}{\beta^2 a_2}}. \tag{28}$$

Case 2. If $q_1 \neq 0,\ a_2\beta \neq 0,\ q_2 = q_3 = 0,\ a_1 = \frac{1}{3}(a_2 + 3a_3),\ q_1(a_4 + \gamma + (a_1 - a_2)\delta) > 0$ and $a_2(a_4 + \gamma + (a_1 - a_2)\delta) < 0$, then:

$$\mathcal{A}_{1,2} = \pm\sqrt{\frac{a_4 + \gamma + (a_1 - a_2)\delta}{2q_1}},\ m_{1,2} = \pm\sqrt{\frac{-3(a_4 + \gamma + (a_1 - a_2)\delta)}{2\beta^2 a_2}}. \tag{29}$$

Case 3. If $q_1 = q_3 = 0,\ q_2 \neq 0, a_2\beta \neq 0, a_1 = \frac{1}{2}(a_2 + 2a_3),\ q_2(a_4 + \gamma + (a_1 - a_2)\delta) > 0$ and $a_2(a_4 + \gamma + (a_1 - a_2)\delta) < 0$, then:

$$\mathcal{A}_{1,2} = \pm\left(\frac{a_4 + \gamma + (a_1 - a_2)\delta}{4q_2}\right)^{\frac{1}{4}},\ m_{1,2} = \pm\sqrt{\frac{-4(a_4 + \gamma + (a_1 - a_2)\delta)}{\beta^2 a_2}}. \tag{30}$$

Case 4. If $q_1q_2 < 0$, $q_3 = 0$, $a_1 = a_2 + a_3$, $\beta a_2 \neq 0$, $a_2q_2 < 0$ and $a_4 + \gamma + (a_1 - a_2)\delta = 0$, then:

$$\mathcal{A}_{1,2} = \pm\sqrt{\frac{-q_1}{2q_2}},\ m_{1,2} = \pm\sqrt{\frac{-q_1^2}{2\beta^2 a_2 q_2}}. \tag{31}$$

According to Case 1 and the formal solution of (27), we can by using the transformation (6) write the kink-type traveling wave solution for the governing model (1) as:

$$\begin{aligned}\psi_{1,2}(t,x) = \mathcal{A}_{1,2}\sqrt{1+\tanh\left(m_{1,2}\left(\tfrac{\alpha}{\Gamma(1+\eta)}t^\eta + \tfrac{\beta}{\Gamma(1+\eta)}x^\eta\right)\right)}\\ \times e^{\left(i\left(\frac{\gamma}{\Gamma(1+\eta)}t^\eta + \frac{\delta}{\Gamma(1+\eta)}x^\eta\right)\right)}.\end{aligned} \tag{32}$$

Using Case 2, we approach the kink-type traveling wave solution for the governing model (1) as follows:

$$\begin{aligned}\psi_{3,4}(t,x) = \mathcal{A}_{1,2}\sqrt{1+\tanh\left(m_{1,2}\left(\tfrac{\alpha}{\Gamma(1+\eta)}t^\eta + \tfrac{\beta}{\Gamma(1+\eta)}x^\eta\right)\right)}\\ \times e^{\left(i\left(\frac{\gamma}{\Gamma(1+\eta)}t^\eta + \frac{\delta}{\Gamma(1+\eta)}x^\eta\right)\right)}.\end{aligned} \tag{33}$$

By utilizing Case 3, we write the kink-type traveling wave solution for the governing model (1) as:

$$\begin{aligned}\psi_{5,6}(t,x) = \mathcal{A}_{1,2}\sqrt{1+\tanh\left(m_{1,2}\left(\tfrac{\alpha}{\Gamma(1+\eta)}t^\eta + \tfrac{\beta}{\Gamma(1+\eta)}x^\eta\right)\right)}\\ \times e^{\left(i\left(\frac{\gamma}{\Gamma(1+\eta)}t^\eta + \frac{\delta}{\Gamma(1+\eta)}x^\eta\right)\right)}.\end{aligned} \tag{34}$$

Finally, according to Case 4, we derive the kink soliton solutions for (1) as follows:

$$\begin{aligned}\psi_{7,8}(t,x) = \mathcal{A}_{1,2}\sqrt{1+\tanh\left(m_{1,2}\left(\tfrac{\alpha}{\Gamma(1+\eta)}t^\eta + \tfrac{\beta}{\Gamma(1+\eta)}x^\eta\right)\right)}\\ \times e^{\left(i\left(\frac{\gamma}{\Gamma(1+\eta)}t^\eta + \frac{\delta}{\Gamma(1+\eta)}x^\eta\right)\right)}.\end{aligned} \tag{35}$$

Figure 8 presents kink wave solution (32) for the governing model (1) on the spatial variable $x \in [-5, 5]$ and the temporal variable $t \in [0, 2]$.

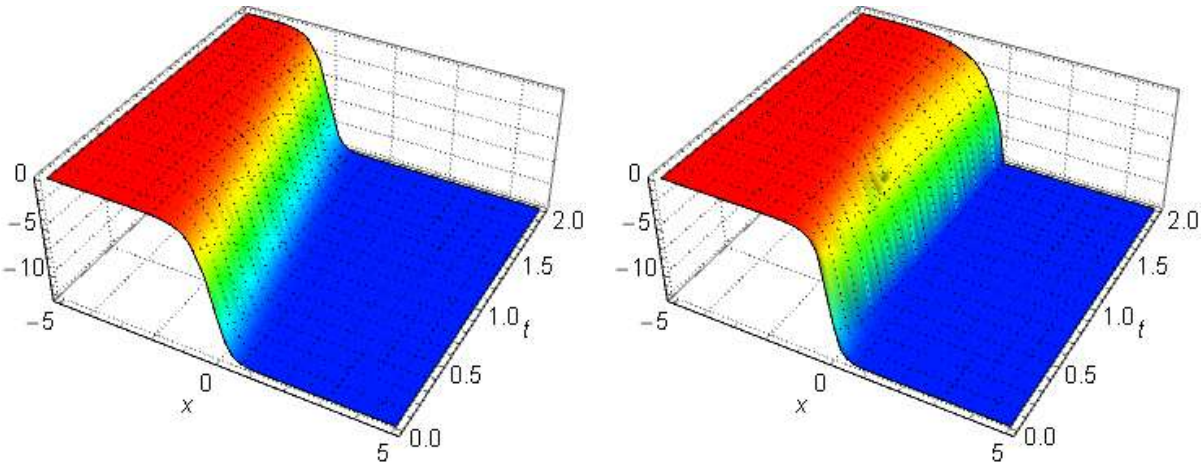

Figure 8. Kink soliton solution $|\psi_1(x,t)|$ in (32) for (1) at $a_1 = 0.1$, $a_2 = 1$, $a_4 = 0.05$, $q_1 = 0.1$, $\alpha = 0.1$, $\beta = 0.1$, $\gamma = 0.1$, $\delta = 3$: (**a**) integer derivative order $\eta = 1$; (**b**) fractional derivative order $\eta = 0.82$.

It is clear from Figure 8 that the kink shape of the surface of the inferred solution (32) was not affected in general, or significantly, when changing the order of the derivative from the integer order, $\eta = 1$, to fractional one, $\eta = 0.82$. To further illustrate the effect of the fractional derivative on the surface of the deduced solutions, we present Figure 9, which shows the two-dimensional plot of the deduced solution (33) at different fractional orders of the derivative:

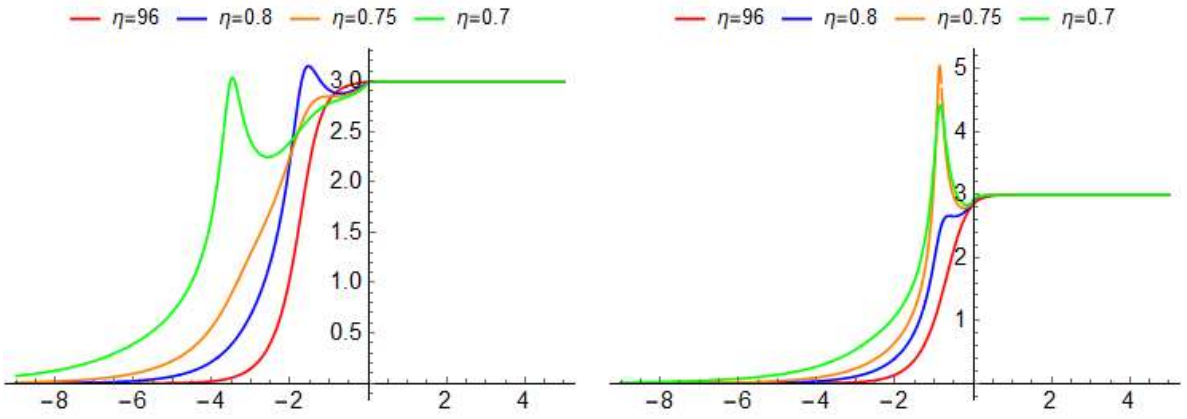

(**a**) (**b**)

Figure 9. Kink soliton solution $|\psi_8(x,t)|$ in (35) where $a_1 = 0.1$, $a_3 = 1$, $q_1 = 0.9$, $q_2 = 0.1$, $\alpha = 0.1$, $\beta = 0.1$, $\gamma = 0.1$, $\delta = 0.1$ at: (**a**) $t = 0.5$; (**b**) $t = 1.5$.

We can notice that the surface structure of the extracted solution (35) is affected by the change in the order of the fractional derivative. It is clear from Figure 9 that the effect was present at the negative values of the spatial variable x, where some perturbations occurred in the kink shape of the solution at certain values of x. In addition to perturbation, it also changes when the value of the temporal variable is changed from $t = 0.5$ to $t = 1.5$.

Moreover, we paid attention to the effect of perturbation parameters a_2 and a_4 on the behavior of the obtained kink soliton solution (33). We observe that when the value of the perturbation parameter a_2 varies from 0.1 to 0.41, then the kink shape of the surface of the obtained solution is getting wider, as shown in Figure 10a. This is exactly the case when the value of the perturbation parameter a_4 increases, then the kink shape of the surface of the obtained solution expands more, see Figure 10b.

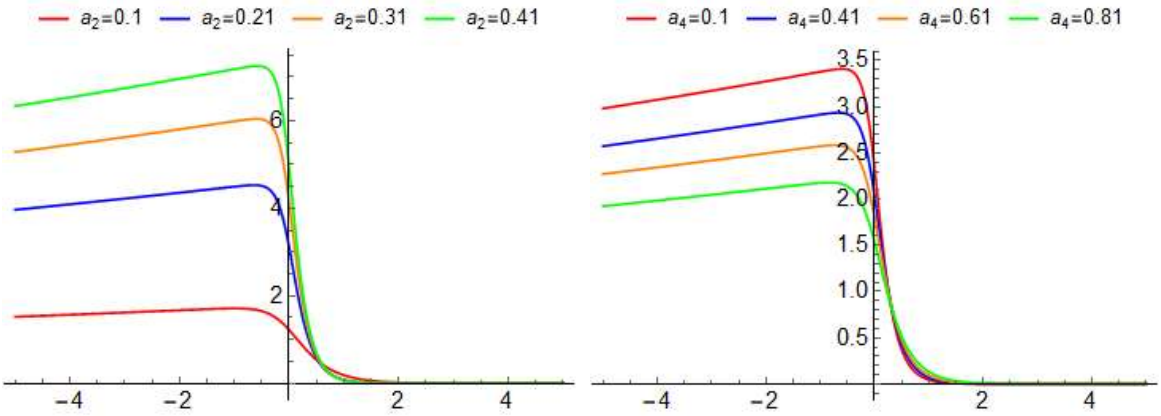

(**a**) (**b**)

Figure 10. Variation of the inferred kink soliton solution $|\psi_4(x,t)|$ in (33) where $t = 0.5$, $a_3 = 0.01$, $q_1 = 0.1$, $\alpha = 0.01$, $\beta = 0.2$, $\delta = 5$, $\gamma = 0.1$ at: (**a**) with the perturbation parameters a_2 and $a_4 = 1$; (**b**) with the perturbation parameters a_4 and $a_2 = 0.1$.

6. Conclusions

In this work, the FCGLE has been considered, which is one of the most notable nonlinear equations in physics that describes the dynamic of the oscillating systems with the parabolic law and weak non-local law nonlinearity. The fractional derivative has been considered in a local approach. Accordingly, we utilized a suitable traveling wave transformation to reduce the governing model into an integer order ordinary differential equation and presented a study on the dynamic behavior of the obtained dynamic system under certain parameter regions. Moreover, two types of soliton solutions, namely, bright and kink solitons, have been established with restrictive conditions to ensure their existence using the ansatz method. The graphical representation has been introduced in 2D and 3D at various values for the parameters with integer and fractional derivative orders to provide a comparison for the physical properties of the constructed solutions at the fractional derivative orders.

Author Contributions: All authors contributed equally to this work. All authors have read and agreed to the published version of the manuscript.

Funding: This research received no external funding.

Data Availability Statement: Not applicable.

Conflicts of Interest: The authors declare no conflict of interest.

References

1. Goyal, A.; Alka; Raju, T.S.; Kumar, C.N. Lorentzian-type soliton solutions of ac-driven complex Ginzburg–Landau equation. *Appl. Math. Comput.* **2012**, *218*, 11931–11937. [CrossRef]
2. Aranson, I.S.; Kramer, L. The world of the complex Ginzburg-Landau equation. *Rev. Mod. Phys.* **2002**, *74*, 99–143. [CrossRef]
3. Hasan, S.; Nadir Djeddi, N.; Al-Smadi, M.; Al-Omari, S.; Momani, S.; Fulga, A. Numerical solvability of generalized Bagley–Torvik fractional models under Caputo–Fabrizio derivative. *Adv. Differ. Equ.* **2022**, *469*, 1–21. [CrossRef]
4. Al-Smadi, M.; Abu Arqub, A. Computational algorithm for solving fredholm time-fractional partial integro dif-ferential equations of dirichlet functions type with error estimates. *Appl. Math. Comput.* **2019**, *342*, 280–294. [CrossRef]
5. García-Morales, V.; Krischer, K. The complex Ginzburg–Landau equation: An introduction. *Contemp. Phys.* **2012**, *53*, 79–95. [CrossRef]
6. Shqair, M.; Alabedalhadi, M.; Al-Omari, S.; Al-Smadi, M. Abundant Exact Travelling Wave Solutions for a Fractional Massive Thirring Model Using Extended Jacobi Elliptic Function Method. *Fractal Fract.* **2022**, *6*, 252. [CrossRef]
7. Sakaguchi, H. Phase dynamics of the coupled complex ginzburg-landau equations. *Prog. Theor. Phys.* **1995**, *93*, 491–502. [CrossRef]
8. Megne, L.T.; Tabi, C.B.; Kofane, T.C. Modulation instability in nonlinear metamaterials modeled by a cubic-quintic complex Ginzburg-Landau equation beyond the slowly varying envelope approximation. *Phys. Rev. E* **2020**, *102*, 042207. [CrossRef]
9. Xu, G.; Zhang, Y.; Li, J. Exact solitary wave and periodic-peakon solutions of the complex Ginzburg–Landau equation: Dynamical system approach. *Math. Comput. Simul.* **2022**, *191*, 157–167. [CrossRef]
10. Yao, S.-W.; Ilhan, E.; Veeresha, P.; Baskonus, H.M. A powerful iterative approach for quintic complex ginzburg–landau equation within the frame of fractional operator. *Fractals* **2021**, *29*, 2140023. [CrossRef]
11. Al-Smadi, M. Fractional residual series for conformable time-fractional Sawada–Kotera–Ito, Lax, and Kaup–Kupershmidt equations of seventh order. *Math. Methods Appl. Sci.* **2021**. *early view*. [CrossRef]
12. Hosseini, K.; Mirzazadeh, M.; Osman, M.S.; Al Qurashi, M.; Baleanu, D. Solitons and Jacobi Elliptic Function Solutions to the Complex Ginzburg–Landau Equation. *Front. Phys.* **2020**, *8*, 225. [CrossRef]
13. Zayed, E.M.; Alngar, M.E.; El-Horbaty, M.; Biswas, A.; Alshomrani, A.S.; Ekici, M.; Yıldırım, Y.; Belic, M.R. Optical solitons with complex Ginzburg-Landau equation having a plethora of nonlinear forms with a couple of improved integration norms. *Optik* **2020**, *207*, 163804. [CrossRef]
14. Zhu, W.; Xia, Y.; Bai, Y. Traveling wave solutions of the complex Ginzburg-Landau equation with Kerr law non-linearity. *Appl. Math. Comput.* **2020**, *382*, 125342. [CrossRef]
15. Salete, E.; Vargas, A.M.; García, Á.; Negreanu, M.; Benito, J.J.; Ureña, F. Complex Ginzburg–Landau Equation with Generalized Finite Differences. *Mathematics* **2020**, *8*, 2248. [CrossRef]
16. Diaz, J.I.; Padial, J.; Tello, J.I.; Tello, L. Complex Ginzburg-Landau equations with a delayed nonlocal perturbation. *Electron. J. Differ. Equ.* **2020**, *40*, 1–18.
17. Matsuda, T. Global well-posedness of the two-dimensional stochastic complex Ginzburg-Landau equation with cubic nonlinearity. *arXiv* **2020**, arXiv:2003.01569, preprint.
18. Hosseini, K.; Mirzazadeh, M.; Baleanu, D.; Raza, N.; Park, C.; Ahmadian, A.; Salahshour, S. The generalized complex Ginzburg–Landau model and its dark and bright soliton solutions. *Eur. Phys. J. Plus* **2021**, *136*, 1–12. [CrossRef]

19. Alneimat, M.; Moakher, M.; Djeddi, N.; Al-Omari, S. Numerical Solution of Fractional Model of Atangana-Baleanu-Caputo Integrodifferential Equations with Integral Boundary Conditions. *J. Appl. Math. E-Notes* **2022**. *to appear*.
20. Hussain, A.; Jhangeer, A.; Abbas, N.; Khan, I.; Sherif, E.S.M. Optical solitons of fractional complex Ginzburg–Landau equation with conformable, beta, and M-truncated derivatives: A comparative study. *Adv. Differ. Equ.* **2020**, *2020*, 612. [CrossRef]
21. Qiu, Y.; Malomed, B.A.; Mihalache, D.; Zhu, X.; Zhang, L.; He, Y. Soliton dynamics in a fractional complex Ginz-burg-Landau model. *Chaos Solitons Fractals* **2020**, *131*, 109471. [CrossRef]
22. Zhang, L.; Zhang, Q.; Sun, H.-W. Exponential Runge–Kutta Method for Two-Dimensional Nonlinear Fractional Complex Ginzburg–Landau Equations. *J. Sci. Comput.* **2020**, *83*, 1–24. [CrossRef]
23. Lu, P.; Wang, B.; Dai, C. Fractional traveling wave solutions of the (2 + 1)-dimensional fractional complex Ginzburg–Landau equation via two methods. *Math. Methods Appl. Sci.* **2020**, *43*, 8518–8526. [CrossRef]
24. Zhang, Q.; Hesthaven, J.S.; Sun, Z.-Z.; Ren, Y. Pointwise error estimate in difference setting for the two-dimensional nonlinear fractional complex Ginzburg-Landau equation. *Adv. Comput. Math.* **2021**, *47*, 1–33. [CrossRef]
25. Lu, H.; Bates, P.W.; Lü, S.; Zhang, M. Dynamics of the 3-D fractional complex Ginzburg–Landau equation. *J. Differ. Equations* **2015**, *259*, 5276–5301. [CrossRef]
26. Huang, C.; Li, Z. New Exact Solutions of the Fractional Complex Ginzburg–Landau Equation. *Math. Probl. Eng.* **2021**, *2021*, 1–8. [CrossRef]
27. Layek, G.C. *An Introduction to Dynamical Systems and Chaos*; Springer: New Delhi, India, 2015; Volume 449.
28. Chow, S.N.; Hale, J.K. *Methods of Bifurcation Theory*; Springer Science & Business Media: Berlin/Heidelberg, Germany, 2012; Volume 251.
29. Singh, S.; Kaur, L.; Sakkaravarthi, K.; Sakthivel, R.; Murugesan, K. Dynamics of higher-order bright and dark rogue waves in a new (2+1)-dimensional integrable Boussinesq model. *Phys. Scr.* **2020**, *95*, 115213. [CrossRef]
30. Singh, S.; Sakkaravarthi, K.; Murugesan, K. Localized nonlinear waves on spatio-temporally controllable back-grounds for a (3 + 1)-dimensional Kadomtsev-Petviashvili-Boussinesq model in water waves. *Chaos Solitons Fractals* **2022**, *155*, 111652. [CrossRef]
31. Sakkaravarthi, K.; Mareeswaran, R.B.; Kanna, T. Engineering optical rogue waves and breathers in a coupled non-linear Schrödinger system with four-wave mixing effect. *Phys. Scr.* **2020**, *95*, 095202. [CrossRef]
32. Alabedalhadi, M.; Alhazmi, S.; Al-Omari, S.; Al-Smadi, M.; Momani, S. Novel bright and kink optical soliton solutions of fractional Lakshmanan-Porsezian-Daniel equation with kerr law nonlinearity in conformable sense. *Fractals* **2022**. *to appear*. [CrossRef]
33. Al-Smadi, M.; Al-Omari, S.; Karaca, Y.; Momani, S. Effective analytical computational technique for conformable time-fractional nonlinear Gardner equation and Cahn-Hillard equations of fourth and sixth order emerging in dispersive media. *J. Funct. Spaces* **2022**. *to appear*.
34. Alaroud, M.; Ababneh, O.; Tahat, N.; Al-Omari, S. Analytic technique for solving temporal time-fractional gas dynamics equations with Caputo fractional derivative. *AIMS Math.* **2022**, *7*, 17647–17669. [CrossRef]
35. Yang, X.-J.; Baleanu, D.; Srivastava, H.M. *Local Fractional Integral Transforms and Their Applications*; Academic Press: Cambridge, MA, USA, 2015. [CrossRef]
36. Das, S. *Functional Fractional Calculus*; Springer Science & Business Media: Berlin/Heidelberg, Germany, 2011.
37. Sabatier, J.; Agrawal, O.P.; Machado, J.A.T. *Advances in Fractional Calculus: Theoretical Developments and Ap-plications in Physics and Engineering*; Springer: New York, NY, USA, 2007. [CrossRef]
38. Kilbas, A.A.; Srivastava, H.M.; Trujillo, J.J. *Theory and Applications of Fractional Differential Equations*; Elsevier: Amsterdam, The Netherlands, 2006; Volume 204.
39. Baskonus, H.; Ruiz, L.S.; Ciancio, A. New Challenges Arising in Engineering Problems with Fractional and Integer Order. *Fractal Fract.* **2021**, *5*, 35. [CrossRef]
40. Guner, O.; Bekir, A. Exact solutions to the time-fractional differential equations via local fractional derivatives. *Waves Random Complex Media* **2018**, *28*, 139–149. [CrossRef]
41. Jia, Z.; Hu, M.; Chen, Q.; Jai, S. Local fractional differential equations by the Exp-function method. *Int. J. Numer. Methods Heat Fluid Flow* **2015**, *25*, 1845–1849. [CrossRef]
42. Bataiha, I.; Momani, S.; Quannas, A.; Momani, Z.; Hadid, S. Fractional-order COVID-19 pandamic outbreak: Modeling and stability analysis. *Int. J. Biomath.* **2022**, *15*, 2150090. [CrossRef]
43. He, J.-H.; Elagan, S.; Li, Z. Geometrical explanation of the fractional complex transform and derivative chain rule for fractional calculus. *Phys. Lett. A* **2012**, *376*, 257–259. [CrossRef]
44. Saha, A. Bifurcation of travelling wave solutions for the generalized KP-MEW equations. *Commun. Nonlinear Sci. Numer. Simul.* **2012**, *17*, 3539–3551. [CrossRef]
45. Zhang, B.; Xia, Y.; Zhu, W.; Bai, Y. Explicit exact traveling wave solutions and bifurcations of the generalized com-bined double sinh–cosh-Gordon equation. *Appl. Math. Comput.* **2019**, *363*, 124576. [CrossRef]
46. Al-qudah, Y.; Alaroud, M.; Qoqazeh, H.; Jaradat, A.; AlHazmi, S.; Al-Omari, S. Approximate Analytic-Numeric Fuzzy Solutions of Fuzzy Fractional, Equations Using Residual Power Series Approach. *Symmetry* **2022**, *14*, 804. [CrossRef]

47. Alabedalhadi, M.; Al-Smadi, M.; Al-Omari, S.; Momani, S. New optical soliton solutions for coupled resonant Davey-Stewartson system with conformable operator. *Opt. Quantum Electron.* **2022**, *54*, 392. [CrossRef]
48. Hasan, S.; Harrouche, N.; Al-Omari, S.K.Q.; Al-Smadi, M.; Momani, S.; Cattani, C. Hilbert solution of fuzzy fractional boundary value problems. *Comput. Appl. Math.* **2022**, *41*, 1–22. [CrossRef]